

> REPLACE THIS LINE WITH YOUR MANUSCRIPT ID NUMBER (DOUBLE-CLICK HERE TO EDIT) <

Identification of Damaged Waterproofing Layer for Patch Antenna Sensor Embedded in Cement Paste

Zhuoran Yi, Kangqian Xu, Songtao Xue, Miao Cao, Liyu Xie, Jonathan Monical, Xianzhi Li, and Kang Jiang

Abstract—A waterproofing layer is necessary to maintain the performance of a patch antenna sensor, especially when embedded in a wet environment. The influence of varying levels of damaged waterproofing layers on the accuracy and sensitivity of sensors has been analyzed in this paper. The behavior of a patch antenna sensor with a possible damaged waterproofing layer is described by an equivalent model with a covered dielectric load. Theoretical calculation and simulation in HFSS ver.15 have been utilized to confirm the influence of the leakage. The antenna sensor with a damaged waterproofing layer tends to have a smaller initial resonant frequency and poor accuracy. Considering three antenna sensors with undamaged, half-damaged, and fully damaged waterproofing layers, an experiment is conducted to verify the influence of damage on sensor performance. Compared with the undamaged waterproofing layer case, the case with a fully damaged waterproofing layer has an initial resonant frequency that is 50% smaller, and the error increases from 10% to 33%. The identification method for the damaged condition of the waterproofing layer is summarized based on the irregularity of the return loss (S11) and resonant frequency.

Index Terms—Patch antenna; Damaged waterproofing layer; Leakage; Setting time detection.

This research was funded by the National Natural Science Foundation of China (Grant Nos. 52408339, 52378311 and 52178298), the Natural Science Foundation of Shandong Province (ZR2024QE159), and the Natural Science Foundation of Qingdao City (24-4-4-zrjj-71-jch). Best thanks to Dr. Wu and Dr. Chen for the good advice. (Corresponding author: Kang Jiang.)

Zhuoran Yi is with the Department of Disaster Mitigation for Structures, Tongji University, Shanghai 200092, China (e-mail: linsmyk@gmail.com).

Kangqian Xu and Xianzhi Li are with the School of Civil Engineering, Qingdao University of Technology, Qingdao, China (e-mail: 727489206@qq.com, lixianzhi@qut.edu.cn).

Songtao Xue with the Department of Disaster Mitigation for Structures, Tongji University, Shanghai 200092, China, State Key Laboratory of Disaster Reduction in Civil Engineering, Shanghai 200092, and Department of Architecture, Tohoku Institute of Technology, Sendai 982-8577, Japan (e-mail: xue@tongji.edu.cn).

Miao Cao is with the Department of Architecture, Tohoku Institute of Technology, Sendai 982-8577, Japan (e-mail: caomiao@toitech.ac.jp)

Liyu xie is with the Department of Disaster Mitigation for Structures, Tongji University, Shanghai 200092, China, College of Civil Engineering and Architecture, Xinjiang University, Urumqi, 830046, China, and State Key Laboratory of Disaster Reduction in Civil Engineering, Shanghai 200092, China (e-mail: liyuxie@tongji.edu.cn).

Jonathan Monical is with the Department of architecture and building science, Tohoku University, Sendai, 980-8579, Japan (e-mail: jmonical@rcl.archi.tohoku.ac.jp)

Kang Jiang is with the College of Engineering, Ocean University of China, Qingdao 266100, China, Department of Disaster Mitigation for Structures, Tongji University, Shanghai 200092, China (e-mail: jk1118@tongji.edu.cn)

I. INTRODUCTION

THE health monitoring of reinforced concrete (RC) elements related to measuring deformation, humidity, setting time, and temperature is becoming more common in the stages of construction and maintenance [1]–[6]. Patch-antenna-based sensors are potential tools for identifying the internal conditions of cement-based materials [7]–[12]. Nevertheless, as shown in Fig 1(a), because the antenna sensor is sensitive to the dielectric medium (cement) and conductor (rebar) in the near field [13]–[15], the complex electromagnetic environment of cement-based materials, especially during the hydration stage, will produce noise in measurements and significantly decrease testing accuracy [16], [17].

The waterproofing layer has been designed to maintain reasonable performance of the antenna sensor embedded in wet environments including human skin [18], clothing [19], and cement-based material [20]–[22]. Focusing on the cement-based material, the waterproofing layer is necessary for embedded antenna sensors [23], [24]. Two basic concepts with different waterproofing layers are shown in Fig. 1(b).

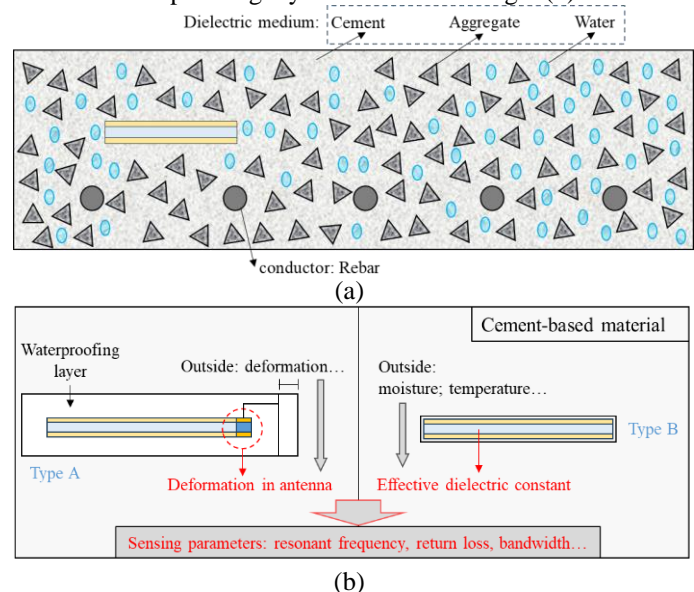


Fig. 1. Configuration of antenna sensor embedded in concrete (a) embedded environment considering dielectric medium (cement, aggregate, water) and conductor (rebar) (b) types of normally embedded antenna sensor for deformation or condition sensing.

Type A configuration detects relative deformation or movement of the antenna sensor [23], [25]. The environment

> REPLACE THIS LINE WITH YOUR MANUSCRIPT ID NUMBER (DOUBLE-CLICK HERE TO EDIT) <

is expected to not affect the accuracy of the sensor because the waterproofing layer is thick enough to provide a constant electromagnetic environment at the near field of the antenna sensor. Type B configuration detects the condition of the cement-based material, such as temperature, setting time, and moisture content, utilizing the shift of the effective dielectric constant of the antenna sensor as the sensing parameter [24], [26]–[28]. The sensing range is within the near field of the antenna which needs to be as thin as possible relative to the cement-based material to enlarge the influence of the varying dielectric constant.

Type B configuration is likely to result in failure of the waterproofing layer because of the thin design which produces leakage inside the sensor package. Because the leak will allow water to attach to the surface of the sensor and produce errors in measurements, the influence of the leakage should be investigated. It is also necessary to identify the possible damage causing the leakage to the waterproofing layer. Though waterproofing is widely utilized as part of the encapsulation of sensors, the entire influence of the damage to the waterproofing layer is not fully investigated.

This research would like to quantitatively identify the influence of a damaged waterproofing layer on the accuracy and sensitivity of the embedded patch antenna sensor, further summarizing the identification method for the possible damage of the waterproofing layer in the practical utilization. Since the detection of the dielectric constant is the main working principle of the embedded patch antenna sensor, mainly the influence of the dielectric medium is taken into consideration in this paper. It should be noted that the influence of the conductor (rebar) is mainly concentrated on the interrogation and will be investigated in the future. Water leakage is regarded as the main effect of the damaged waterproofing layer. Instead of all embedded sensor types, an antenna sensor for the setting time detection in Ref. [26] is selected as a sample to simplify the analysis. The theoretical calculation was first utilized to identify the type and degree of possible leakage. The leaked water introduced by the damaged waterproofing layer is equivalent to an extra dielectric layer covered on the antenna. The change of resonant frequency is utilized for the detection of setting time. The variation of accuracy and sensitivity caused by the extra layer is calculated by transforming the electrostatic field region of the above area of the patch antenna sensor into the interior of a rectangle according to the conformal mapping. After that, the simulation in High-Frequency Structure Simulator (HFSS) ver.15 [27] is utilized to evaluate the influence quantitatively. Experiments are finally carried out to confirm the influence, considering three specimens with perfect, half-broken, and no (corresponding to totally damaged one) waterproofing layer. The possible detecting way for the damage of the waterproofing layer is finally summarized. This analysis is expected to improve the feasibility of the embedded patch antenna sensors.

This paper is arranged as follows: Section 2 theoretically analyzes the influence of the possible damage in the waterproofing layer using the conformal mapping; Section 3 identifies the influence quantitatively based on the simulation in HFSS ver.15. In Section 4, an experiment with a

waterproofing layer under different damaged conditions has further confirmed the influence. The possible detection method for the waterproof damage has been summarized and verified in Section 4. Finally, the conclusion is drawn, and the potential research in the future is clarified.

II. METHODOLOGY

The influence of the damaged waterproofing layer is first investigated here quantitatively. All the sensors of type B will share the same sensing mechanism. To simplify the analysis, only a patch antenna sensor utilized for setting time detection is considered an example [26]. As the most popular sensing parameter, the resonant frequency is selected instead of the multi-electromagnetic parameters [28]. Because of the wettest and most complex inside environment, cement paste is chosen as the detecting material in this paper. It should be noted that this analysis can work not only for the setting time detection using resonant frequency but also for other conditions, such as the detection of humidity and temperature by bandwidth or radiation efficiency, because of a similar mechanism [29].

In this section, the working principle of the patch antenna sensor for setting time is clarified first. After that, the damaged waterproof's possible influence on the sensor's effectiveness is clarified, followed by a quantitative study of the sensitivity and the proposal for the identification of the damaged waterproofing layer.

A. Working principle for the embedded antenna sensor

One of the simplest forms of the setting time sensor with a dielectric constant ϵ_1 for the dielectric board is shown in Fig. 2 [26]. The waterproofing layer, which is a dielectric medium, is not considered here because of its physically thin size (0.05 mm). The height of the radiation patch h_{co} is 0.035 mm (1 oz). Two kinds of materials with dielectric constants ϵ_2 and ϵ_3 surround the antenna sensor, representing the cement paste and air, respectively.

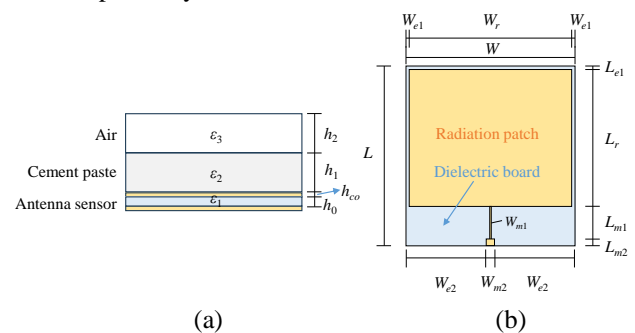


Fig. 2. Normal patch antenna sensor with covered cement paste and outside air. (a) Front view (b) in-plane view.

The cement paste can be regarded as a mixture of water (liquid), air, and cement under hydration (solid). Hence, the dielectric constant of cement paste should be evaluated by a mixing model. Several mixing models have been proposed by Sihvola [30], Wiener [31], and Birchak [32], have been proposed. In this paper, the model of Birchak is utilized for the calculation of the dielectric constant of cement, since it is

> REPLACE THIS LINE WITH YOUR MANUSCRIPT ID NUMBER (DOUBLE-CLICK HERE TO EDIT) <

proposed directly for the calculation of the soil, which shares similar mixing states with cement paste. The complex permittivity of the cement ε_{2-d} is determined by the moisture content, as described in Eq. 1 [33], [34].

$$\varepsilon_{2-d}^{0.5} = R_w \varepsilon_{w-d}^{0.5} + (1 - R_w) \varepsilon_{s-d}^{0.5}, \quad (1)$$

where R_w is the volume fraction of the water inside the cement paste. ε_{w-d} and ε_{s-d} are the complex permittivity of water and the solid part of the cement, which is set as 82 (15 °C) [35] and 5 [26] respectively. The dielectric constant of cement is obtained from the real part of the output of Eq. 1. The effective dielectric constant of the patch antenna ε_e is influenced by the nearby dielectric medium, based on Eq. 2 [28].

$$\varepsilon_e = \varepsilon_1 q_{1n} + \frac{\varepsilon_1 (1 - q_{1n})^2 \times [\varepsilon_2^2 q_{2n} q_3 + \varepsilon_2 \varepsilon_3 (q_{2n} q_4 + (q_3 + q_4)^2)]}{\varepsilon_2^2 q_{2n} q_3 q_4 + \varepsilon_1 (\varepsilon_2 q_3 + \varepsilon_3 q_4) (1 - q_{1n} - q_4)^2 + \varepsilon_2 \varepsilon_3 q_4 [q_{2n} q_4 + (q_3 + q_4)^2]}, \quad (2)$$

where q_{1n} , q_{2n} , q_3 , and q_4 are the effect factors for the dielectric board, water layer, covered cement, and air, respectively. Especially, q_3 has been revised for the error caused by the overestimation of the top layer of the model (which is the covered cement and air) [36]. Based on the reference [26], the influence of the dielectric constant and the location of the covering material can be summarized as follows: 1). Dielectric constant. With the increase of the dielectric constant of covering material, the equivalent dielectric constant of dielectric board will increase due to the fringe effect. 2). Location. The material near the radiation patch will cause a larger fringe effect than the material far from the radiation patch.

Considering the effective dielectric constant, the resonant frequency of the antenna sensor is given by Eq. 3.

$$f_0 = \frac{c}{2L_r \sqrt{\varepsilon_e}}, \quad (3)$$

where c is the light speed, ε_1 is the dielectric constant of the board, and L_r is the length of the patch antenna radiation patch. Hence, the resonant frequency can be a parameter for detecting moisture content. As mentioned in Ref.[28]–[29], the setting time of cement paste can be obtained at several characteristic points of the moisture content of the cement. Detailed speaking, the point when the moisture content starts to decrease is the initial setting, and the point with a maximum change rate of the moisture content is regarded as the final setting, as defined in Eq. 4.

$$g(t_{fin}) > g(t_{fin} \pm \Delta t) \quad \Delta t \in R, \quad (4)$$

$$g(t) = f'(t), \quad (5)$$

where t_{fin} is the final setting time, and Δt is the time step. $g(t_{fin})$ is the change rate of moisture constant, which is equal to the differential coefficient of the moisture content $f(t)$ in Eq. 5. Since the resonant frequency is confirmed to have a nearly linear relationship with the moisture content of the cement paste [26], the setting time detection can be done using the measured resonant frequency as the sensing parameter instead of moisture content.

B. Possible effects introduced by damaged waterproof

1) Basic equivalent model

As shown in Fig. 3, two effects will be introduced by the

damaged waterproofing layer. One is the change in the distribution of the nearby dielectric medium. The possible leakage will introduce extra water on the surface of the radiation patch randomly based on the damage place. Another one is the prevention of hydration and evaporation. Compared with the water outside the waterproofing layer, the leaked water inside the layer is hard to participate in the hydration and evaporation.

Combining the two effects mentioned above, the antenna sensor with a damaged waterproofing layer is equivalent to a theoretical model in Fig. 4.

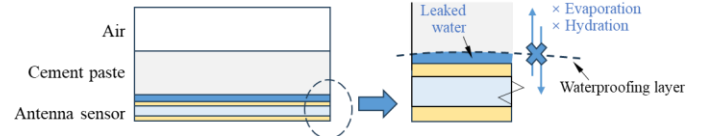


Fig. 3. Concept of influence of leakage caused by damaged waterproofing layer to the evaporation and hydration of the water.

Compared with the original model in Fig. 2, the updated model set an extra water layer between the cement and the patch antenna. During the detection for the setting time, it is regarded as a constant layer according to the early stage of cement hydration due to the prevention effect of evaporation and hydration. The height of the extra layer is determined by the level of the damage. The dielectric constant of the extra layer ε_{ext} is set equal to water ($\varepsilon_{ext} = \varepsilon_w = 82$). Considering the effects of the extra layer, an updated effective dielectric constant ε_{eu} is defined and calculated based on Eq.6 according to reference [33].

$$\varepsilon_{eu} = f(\varepsilon_1, \varepsilon_{ext}, \varepsilon_2, \varepsilon_3, q_{1n}, q_{eu}, q_{2n}, q_{3n}, q_4), \quad (6)$$

where q_{ext} is the effect factor for the extra layer.

Since the extra layer will have a larger dielectric constant and a closer location compared with the cement paste, the fringe effect caused by the extra layer will be much stronger. Therefore, when an extra water layer existed, the change in the dielectric constant of the cement layer farther from the patch antenna has a relatively reduced effect on the resonance frequency of the patch antenna, resulting in a decreased sensitivity of the detection. This effect is further verified by theoretical calculation in the next section.

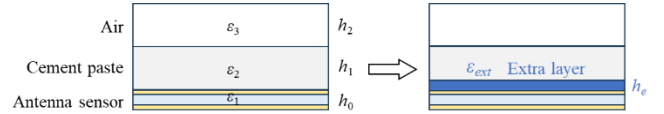


Fig. 4. Equivalent theoretical model of antenna sensor with leakage considering damaged waterproofing layer (front view).

2) Influence of the extra layer

The influence of the extra layer is discussed based on the equivalent model mentioned above. The height of the extra layer h_e is set as an index to describe the level of the damaged waterproofing layer. Considering the case with the parameters of the antenna sensor and cement listed in Tab. I, the influence of the possible leakage on the effective dielectric constant and fundamental resonant frequency f_f of the antenna sensor is shown in Fig. 5.

The dielectric constant of the cement paste ε_2 is set as 14 corresponding to the state before initial setting [26]. With the

> REPLACE THIS LINE WITH YOUR MANUSCRIPT ID NUMBER (DOUBLE-CLICK HERE TO EDIT) <

height of the extra layer increased from 0 to 0.5 mm, the updated effective dielectric constant ϵ_{eu} increased from 2.49 to 2.68, causing the initial resonant frequency to vary from 1.86 to 1.8 GHz.

Besides, the initial resonant frequency remains nearly constant after the height of the extra layer achieving 0.4 mm, indicating the maximum influence of height can be set at the nearby region of 0.4 mm. Hence, in the following analysis, the maximum height is set as 0.5 mm to simplify the calculation. It should be noted that the real height of the water layer remains unknown and may be larger than 0.5 mm.

TABLE I

PROPERTIES OF ANTENNA SENSOR AND CEMENT.

Parameters	W	W_r	L	L_r	h_0	h_1	h_e
Value (mm)	60	50	67	50	0.254	10	0~0.5
Parameters	ϵ_1	ϵ_2	ϵ_3	ϵ_{ext}	h_{co}		
Value	2.2	14~6	1	82	1oz		

where W is the width of the antenna, and h_0 is the height of the dielectric board.

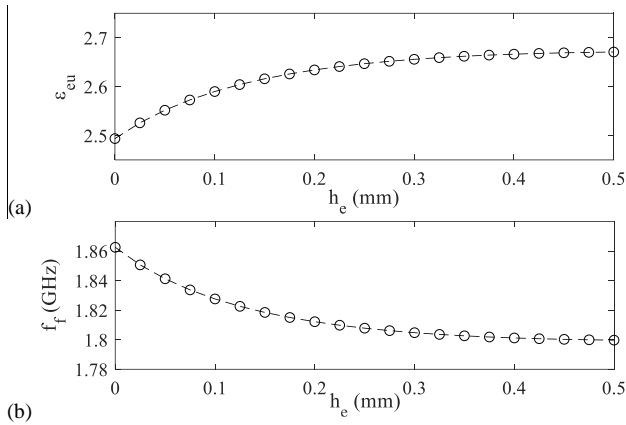


Fig. 5. Influence of the leakage caused by damaged waterproofing layer to (a) updated effective dielectric constant ϵ_{eu} and (b) fundamental resonant frequency f_f .

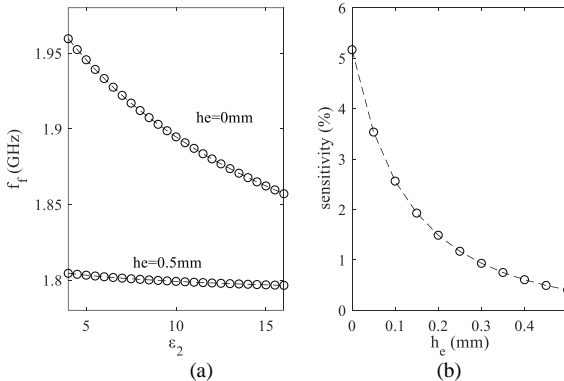


Fig. 6. Influence of the leakage caused by damaged waterproofing layer on the sensitivity (a) resonant frequency - ϵ_2 (b) sensitivity - h_e .

The influence on the sensitivity S defined in Eq. 7 is then analyzed. The dielectric constant of the cement is shifted from 14 to 6, corresponding to the state before the initial setting and after the final setting. As Fig. 6 shows, the sensitivity varied

from 5 % to 0.4 %, with the height of the extra layer increased from 0 to 0.5 mm.

$$S = \left| \frac{f_i - f_f}{f_0} \right|, \quad (7)$$

where f_0 is the original fundamental resonant frequency. f_i , and f_f are the fundamental resonant frequency at the initial and final settings, respectively. In summary, the increase in the extra layer's height will decrease the fundamental resonant frequency and sensitivity at a considerable rate.

3) Possible effects

Several indexes have been considered to evaluate the influence of leakage. The first one E_r , as defined in Eq. 8, is related to the readability of the antenna sensor.

$$E_r = |f_{in-d} - f_{in-n}| / f_{in-n}, \quad (8)$$

where f_{in-d} and f_{in-n} are the detected initial values of the fundamental resonant frequency from the sensor with and without a damaged waterproofing layer, respectively.

Another index, E_a , is set corresponding to the accuracy of the detected setting time.

$$E_a = |t_d - t_n| / t_n, \quad (9)$$

where t_d and t_n are the setting time measured from the sensor with and without a damaged waterproofing layer, respectively.

The final index E_s is proposed to evaluate the sensitivity of the antenna sensor.

$$E_s = |f_{f-m} - f_{in-m}| / f_{in-m}, \quad (10)$$

where f_{f-m} and f_{in-m} are the resonant frequencies at the initial and final setting time, respectively. As shown in Fig.7, the following states are expected to be seen:

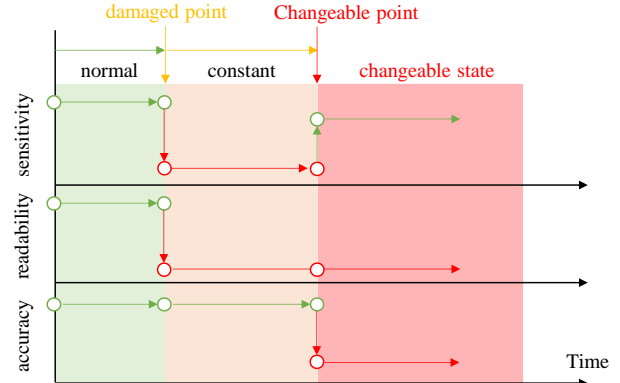


Fig. 7. State of influence of the damaged waterproofing layer, considering accuracy, readability, and sensitivity of the sensor.

1). **Damage point**: the leaked water due to the damaged waterproofing layer will form an extra layer.

2). **Constant state**: this state refers to the entire retardation period and a short period following it. During the induction period, the hydration is stopped, causing a constant water amount. After that, since the water-cement ratio is much larger than the upper part due to the concentration of water, the consumed water can be roughly ignored directly after the induction period. Hence, in this state, the extra layer will remain constant, seriously decreasing the sensitivity and readability of the antenna sensor. However, since the extra layer is constant, the change tendency of the resonant frequency will not be affected. Hence, the accuracy will not

> REPLACE THIS LINE WITH YOUR MANUSCRIPT ID NUMBER (DOUBLE-CLICK HERE TO EDIT) <

decrease.

3). **Changeable point:** with the progress of hydration and evaporation, the height of the extra layer starts to decrease due to the decrease in the moisture content of the cement paste. It should be noted that the change does not happen suddenly but within a time range, and the changeable point is an equivalent state for this phenomenon. The point should be slower than the initial setting but faster than the final setting since the cement will lose much water between the initial and final setting.

4). **Changeable state:** with the decrease in the height of the extra layer, the resonant frequency will increase, which seems to increase the sensitivity. However, it should be noted that the increase in the resonant frequency is not due to the finish of the initial setting or the coming of the final setting. Hence, the resonant frequency change cannot be utilized to detect the setting time, which means the accuracy will decrease in this state.

C. Proposal of identification way for possible leakage

Based on the influence of leakage, two main things are expected to be the indexes for the identification of possible leakage:

- 1) Huge change in the initial resonant frequency.
- 2) Abnormal setting time value and antenna's signal.

To further confirm the proposed characteristics and identification way, a detailed simulation in HFSS ver.15 is carried out in Section 3, followed by experiments in Section 4.

III. SIMULATION

Based on the same setting of Tab. I, a simulation in HFSS ver.15 is proposed to verify the theoretical calculation of the sensitivity and initial resonant frequency in Section 2.

A. Setup of Simulation in HFSS ver.15

Considering the error for the equivalent boundary, a simulated model is established in HFSS ver.15 for further verification based on the parameter setting in Tab. I. The concept is shown in Fig. 8(a). RT/duroid® 5880 laminate is utilized as the dielectric board material. A block with a changeable dielectric constant set on the rectangular patch antenna represents the cement paste. The whole model is fed by a wave port (driven modal), with the input as a time-harmonic voltage signal with an amplitude of 1V. An air box is set to contain the whole model. The length of the air box is larger than a quarter wavelength of the antenna, considering the needs of the simulator under far-field radiation.

The electric field is mainly concentrated at the top and bottom part of the radiation patch, as illustrated in Fig. 8(b). To clearly show the impact of leakage, we intentionally introduced simulated damage in these areas where the electric field is most concentrated, as these regions are expected to have a greater influence on the antenna sensor's performance.

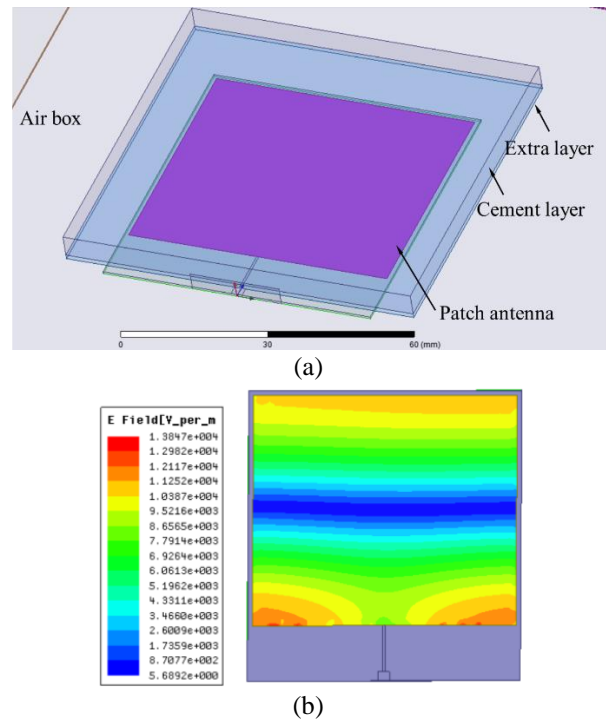


Fig. 8. Concept of the simulated antenna sensor (a) model setup (b) electric field distribution at 1.92 GHz (with a load of cement paste, dielectric constant of cement = 6).

B. Results and discussion

With the dielectric constant of the dielectric board shifting from 14 to 6, the S_{11} curve of the patch antenna is shown in Fig. 9. The height of the extra layer is set constant as 0mm for Fig. 9(a) and 0.5mm for Fig. 9(b), corresponding to the case without and with possible damage in the waterproofing layer. With the variation in parameters of the water layer, the Q factor of the antenna sensor is measured and confirmed to be at least 30, demonstrating that the proposed sensor remains detectable during practical utilizations.

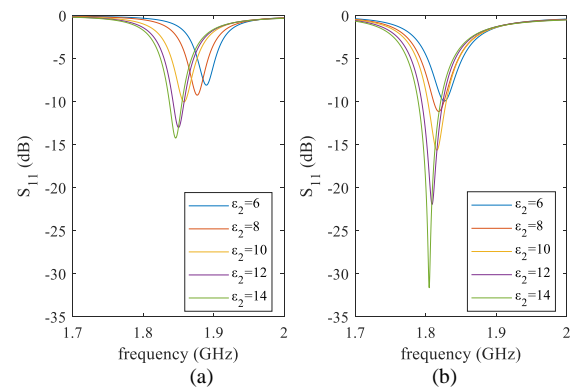


Fig. 9. S_{11} curve with the dielectric constant of covering material ϵ_2 varied from 6-14 (a) $h_e=0$ mm (b) $h_e=0.5$ mm.

> REPLACE THIS LINE WITH YOUR MANUSCRIPT ID NUMBER (DOUBLE-CLICK HERE TO EDIT) <

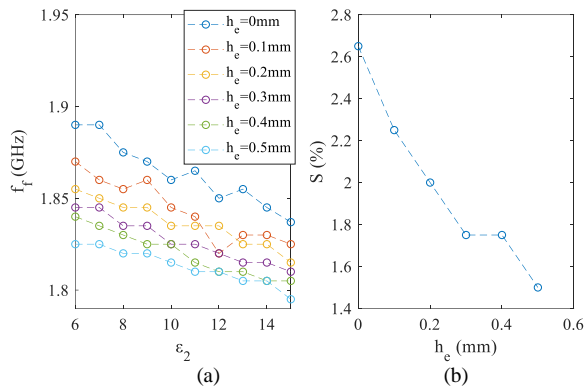


Fig. 10. Influence of the extra water layer (a) Resonant frequency under the change in the dielectric constant of the dielectric board and height of the extra layer (b) sensitivity - h_e .

Though the S_{11} has no huge difference, the value of both resonant frequency f_r and sensitivity S decreases obviously with the setting of an extra layer.

The resonant frequency value is then selected from the minimum value of the S_{11} curve. Similar to the analysis in Section 2.B.2, the resonant frequency is plotted in Fig. 10. As the dielectric constant of the dielectric board shifts from 14 to 6 and the height of the extra layer increases from 0 to 0.5 mm, the total change in resonant frequency decreases from 0.05 GHz to 0.03 GHz. The sensitivity decreases by about 40% when the height of the extra layer increases to 0.5mm, which indicates that slight damage in the waterproofing layer may greatly influence the detecting accuracy.

C. Identification of the damaged state of the waterproofing layer

Based on the effects analyzed in Sections 2 and 3, the following characteristics can be utilized to identify potential leakage introduced by a damaged waterproofing layer:

- 1). Serious decrease of the initial resonant frequency.
- 2). Resonant frequency remains constant for a long time.
- 3). The detected initial setting time will be close to the detected final setting time (e.g., within 30 minutes).
- 4). S_{11} has a huge variation compared with the normal case.

IV. EXPERIMENT

An experiment is designed to check the influence of the damaged waterproofing layer. The initial resonant frequency, testing accuracy, and sensitivity of each specimen are compared first, followed by the verification of the method to identify the damage.

A. Experiment setup

With the design shown in Tab. II, the utilized three antennas with waterproofing layers under different damage conditions are fabricated, as shown in Fig. 11.

The patch antenna is positioned at the bottom of the cement, with the initial gap between the cement and the antenna sensor considered as the thickness of the waterproofing layer. Cement with grade P1.42.5 is utilized to fabricate cement paste under normal consistency with a water-cement ratio of 1:3 [37].

TABLE II
DESIGN OF THREE SPECIMENS WITH DIFFERENT DAMAGE.

Type	Waterproofing layer	Damage
① No damage	Two layers of plastic wrap	No
② Part damage	One layer of plastic wrap	Several holes
③ Full damage	No plastic wrap	Remove

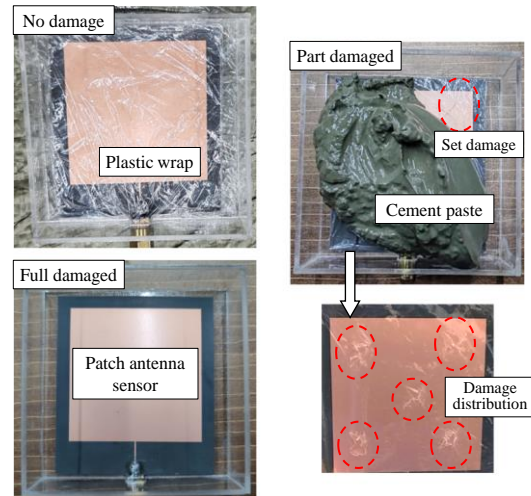


Fig. 11. Pictures of the manufactured designs described in Tab. II. Top-left corner (no damage), right (part damage), and bottom-left corner (full damage).

The accurate initial and final setting times are given by the standard penetration test using a Vicat apparatus. The testing environment is kept constant during the experiment by the air conditioner, as listed in Tab. III. A Vector Network Analyzer (VNA, Rohde & Schwarz – Munich, Germany) is utilized to interrogate antenna sensors and obtain the S_{11} curves by coaxial measurements, and the results are discussed in Section 4.B. Before observation, short, open, load, and through standards are sequentially connected to the VNA ports to define the reference plane and remove systematic errors.

TABLE III
PARAMETERS OF PACKAGE AND TESTING CONDITION.

Parameters	Dimension (mm ³)	Cement height (mm)	Temperature (C)	Humidity (%)
Value	74 x 74 x 20	15	15	41

B. Data analysis

1). Standard penetration test

Corresponding to each specimen, standard penetration tests have been done every 10 minutes. The results of the standard penetration test are shown in Tab. IV. Two states are considered: 1). At 130 minutes: the penetration depth of the test needle is less than 67 mm, indicating that the cement has developed a certain level of strength and has entered the initial setting stage. 2). At 200 minutes: the test needle no longer leaves a scar on the cement, demonstrating that the cement has developed sufficient strength and has reached the final setting stage.

Since the environmental conditions and water-cement ratio remained the same for each group, the obtained setting time is the same among the three groups, which is 130 min for the

> REPLACE THIS LINE WITH YOUR MANUSCRIPT ID NUMBER (DOUBLE-CLICK HERE TO EDIT) <

initial and 230 min for the final setting.

TABLE IV

PENETRATION DEPTH AND STATE OF SCARE OF STANDARD PENETRATION TEST.

Time (min)	~100	120	130	~210	220	230
Penetration depth (mm)	70	68	67	/	/	/
Scar state	/	/	/	clear	not clear	none

2). Detection of setting time

The measured S_{11} curves with smooth filtering for the three specimens are shown in Fig. 12. The resonant frequency is then obtained from the last point of the S_{11} curve and further plotted in Fig. 13. The initial setting time of the cement is determined at the point where the resonance frequency begins to increase.

Subsequently, at each time point t , a time window $[t-\Delta t, t+\Delta t]$ is selected, and the slope of the linear fitting curve of the resonance frequency within this window is used as the change rate at time t . The results are shown in Fig. 14. The final setting time of the cement is determined at the extremum point of the change rate. Δt is set to 40 minutes in this study based on previous reference [28].

TABLE V

RESULTS OF THE OBTAINED SETTING TIME-BASED ON ANTENNA WITH DIFFERENT DAMAGE.

	Vicat	Type①	Type②	Type③
Initial setting time (min)	130	110	160	210
Final setting time (min)	230	220	180	220
Average error (%)	/	9.8	22.4	32.9

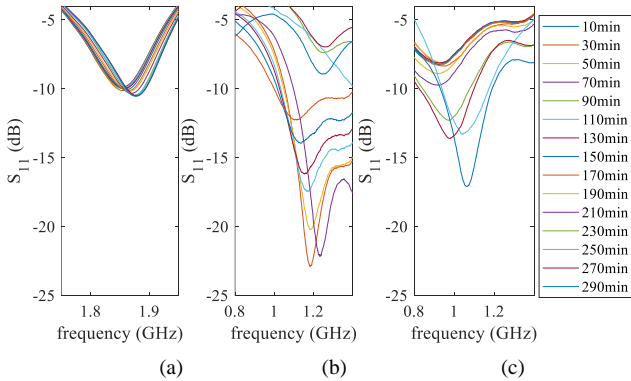


Fig. 12. Change of S_{11} curve of antennas during cement hydration for the specimens (a) no damage (b) part damage (c) full damage.

The detected setting time by patch antenna sensors with different damage types is compared with the standard-setting time measured by the Vicat apparatus, as shown in Tab. V [25]. An error err is defined to compare the accuracy of the antenna sensor, as defined in Eq. 11.

$$err = |t_{an} - t_v| / t_v, \quad (11)$$

where t_{an} and t_v are the setting times detected by the antenna sensor and Vicat apparatus. The initial fundamental resonant frequency, sensitivity, and error are compared in Tab. VI.

With the increase of the damage level, the initial resonant frequency decreases by nearly 50 %, with the error increased from 9.8% to 32.9 %. The sensitivity increases about three times for type ③, while it is meaningless due to the huge detecting error.

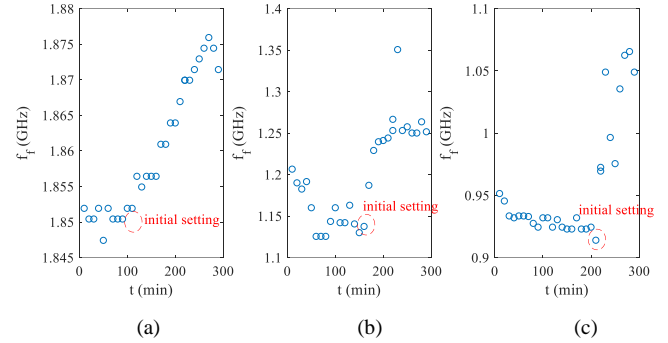


Fig. 13. Change of resonant frequency of antennas during cement hydration for the specimens (a) no damage (b) part damage (c) full damage.

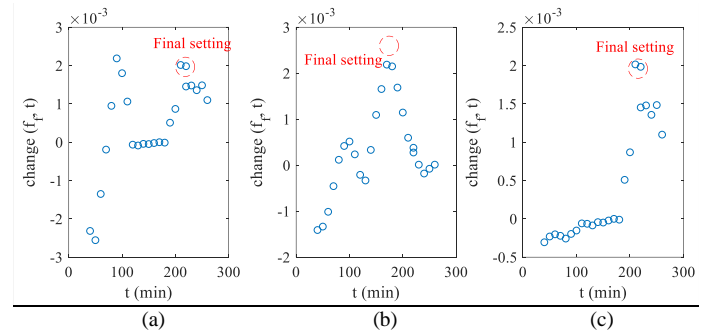


Fig. 14. Change rate of the resonant frequency of antennas during cement hydration for the specimens (a) no damage (b) part damage (c) full damage.

3). Verification of damaged waterproofing layer

Based on the strategy proposed in Section 3. C, the variation of return loss (S_{11}) ΔS and the setting time interval Δt defined in Eqs. 12-13 are summarized in Tab.VI for identifying the damage to the waterproofing layer. Based on previous experiment datasets [26]-[28], the limitations of ΔS and Δt are tentatively designed as 5 dB and 30 min. The damaged case tends to have a large ΔS and a small Δt , which can be the evidence of damage evaluation of the waterproofing layer.

$$\Delta S = |S_{max} - S_{min}|, \quad (12)$$

$$\Delta t = |t_{ini} - t_{fin}|, \quad (13)$$

where S is the minimum value of each S_{11} curve. S_{max} and S_{min} are the maximum and minimum values among the dataset S . t_{ini} and t_{fin} are the initial and final setting times, respectively. The case with a large ΔS and small Δt is supposed to have a damaged waterproofing layer. The identified results corresponding to the three types of antenna sensors are listed in Tab. VII.

Influenced by the damaged waterproofing layer, the basic trend of the change of sensitivity and initial resonant frequency remained the same, indicating the proposed detecting method of damage is effective. More experiments are expected to be carried out to verify detailed influence, such

> REPLACE THIS LINE WITH YOUR MANUSCRIPT ID NUMBER (DOUBLE-CLICK HERE TO EDIT) <

as the damage location, type of waterproofing layer, and water-cement ratio.

It should be noted that the identification of damage relies on the unusual changes in the dielectric constant caused by leakage. However, since the dielectric constant of cement paste can also be influenced by factors such as temperature variations or the presence of cracks, a more detailed analysis should be conducted after the initial assessment using the proposed method in this paper. Besides, the reasonable value of the limitation still needs to be investigated for the real application. Besides, the identification of damage level also needs to be evaluated based on a better index considering much more complex conditions.

TABLE VI

RELATIONSHIP BETWEEN INITIAL RESONANT FREQUENCY, SENSITIVITY, AVERAGE ERROR AND TYPE OF DAMAGE.

Type	Initial resonant frequency(GHz)	Sensitivity (%)	Average error (%)
① No damage	1.85	0.011	9.8
② Part damage	1.2	0.026	22.4
③ Full damage	0.95	0.032	32.9

TABLE VII

EVALUATION OF DAMAGE LEVELS BASED ON PROPOSED METHODS.

Type	ΔS	Δt	Evaluation
① No damage	0.7	110	No damage
② Part damage	16.1	20	Possible damage
③ Full damage	9.1	10	Possible damage

V. CONCLUSION

This paper has evaluated possible effects and identification methods of the damaged waterproofing layer in a patch antenna sensor embedded in cement paste. Leakage is regarded as the main effect of the damaged waterproofing layer. Three conclusions are drawn as follows:

1. According to the experiment, the damaged waterproofing layer tends to decrease the initial resonant frequency by more than 50%, which will cause a huge problem for the interrogation.

2. Damaged waterproofing layer tends to decrease the detecting accuracy. When the waterproofing layer is damaged, the average error for setting time detection increases from 9.8% to 32.9%. The sensitivity will increase, but it is meaningless because of the great error.

3. The damaged case can be identified based on the variation of return loss (S11) ΔS and the setting time interval Δt . A better identification index is expected to be analyzed in the future.

REFERENCES

[1] H. Melhem and H. Kim, "Damage Detection in Concrete by Fourier and Wavelet Analyses," *J. Eng. Mech.*, vol. 129, no. 5, pp. 571–577, May 2003.

[2] D. Ai, H. Zhu, and H. Luo, "Sensitivity of embedded active PZT sensor for concrete structural impact damage detection," *Constr. Build. Mater.*, vol. 111, pp. 348–357, 2016.

[3] C.-C. Cheng, T.-M. Cheng, and C.-H. Chiang, "Defect detection of concrete structures using both infrared thermography and elastic waves," *Autom. Constr.*, vol. 18, no. 1, pp. 87–92, 2008.

[4] Q. Feng, J. Cui, Q. Wang, S. Fan, and Q. Kong, "A feasibility study on real-time evaluation of concrete surface crack repairing using embedded piezoceramic transducers," *Measurement*, vol. 122, pp. 591–596, 2018.

[5] A. Kocherla and K. V. Subramaniam, "Embedded smart PZT-based sensor for internal damage detection in concrete under applied compression," *Measurement*, vol. 163, p. 108018, 2020.

[6] M. Saleem and H. Gutierrez, "Using artificial neural network and non-destructive test for crack detection in concrete surrounding the embedded steel reinforcement," *Struct. Concr.*, vol. 22, no. 5, pp. 2849–2867, Oct. 2021.

[7] X. Li, S. Xue, L. Xie, and G. Wan, "Simultaneous crack and temperature sensing with passive patch antenna," *Struct. Health Monit.*, p. 14759217231184115, Jul. 2023.

[8] K. H. Teng *et al.*, "Embedded smart antenna for non-destructive testing and evaluation (NDT&E) of moisture content and deterioration in concrete," *Sensors*, vol. 19, no. 3, p. 547, 2019.

[9] F. Fioranelli, S. Salous, I. Ndiip, and X. Raimundo, "Through-the-wall detection with gated FMCW signals using optimized patch-like and Vivaldi antennas," *IEEE Trans. Antennas Propag.*, vol. 63, no. 3, pp. 1106–1117, 2015.

[10] R. Salama and S. Kharkovsky, "An embeddable microwave patch antenna module for civil engineering applications," in *2013 IEEE International Instrumentation and Measurement Technology Conference (I2MTC)*, IEEE, 2013, pp. 27–30. Accessed: Oct. 13, 2023. [Online].

[11] K. Bouzaffour, B. Lescop, P. Talbot, F. Gall e, and S. Rioual, "Development of an embedded UHF-RFID corrosion sensor for monitoring corrosion of steel in concrete," *IEEE Sens. J.*, vol. 21, no. 10, pp. 12306–12312, 2021.

[12] M. Gkantou, M. Muradov, G. S. Kamaris, K. Hashim, W. Atherton, and P. Kot, "Novel electromagnetic sensors embedded in reinforced concrete beams for crack detection," *Sensors*, vol. 19, no. 23, p. 5175, 2019.

[13] K. H. Pan, T. G. Moore, and J. T. Bernhard, "Experimental investigation of microstrip antenna behavior beside lossy dielectric materials," in *IEEE Antennas and Propagation Society International Symposium. 2001 Digest. Held in conjunction with: USNC/URSI National Radio Science Meeting (Cat. No. 01CH37229)*, IEEE, 2001, pp. 470–473. Accessed: Oct. 13, 2023. [Online].

[14] K. H. Pan, J. T. Bernhard, and T. G. Moore, "Effects of lossy dielectric material on microstrip antennas," in *2000 IEEE-APS Conference on Antennas and Propagation for Wireless Communications (Cat. No. 00EX380)*, IEEE, 2000, pp. 39–42. Accessed: Oct. 13, 2023. [Online].

[15] J. Dinkic, M. N. Stevanovic, and A. Djordjevic, "Physical Models for Influence of Substrate Permittivity on the Gain of Microstrip Antennas," *IEEE Trans. Antennas Propag.*, 2023, Accessed: Oct. 13, 2023.

[16] K. M. Shams and M. Ali, "Wireless power transmission to a buried sensor in concrete," *IEEE Sens. J.*, vol. 7, no. 12, pp. 1573–1577, 2007.

[17] G. S. Mauro, G. Castorina, A. F. Morabito, L. Di Donato, and G. Sorbello, "Effects of lossy background and rebars on antennas embedded in concrete structures," *Microw. Opt. Technol. Lett.*, vol. 58, no. 11, pp. 2653–2656, Nov. 2016.

[18] J. Oh *et al.*, "Air-Permeable Waterproofing Electrocardiogram Patch to Monitor Full-Day Activities for Multiple Days," *Adv. Healthc. Mater.*, vol. 11, no. 12, p. 2102703, Jun. 2022.

[19] S. Wen, H. Heidari, A. Vilouras, and R. Dahiya, "A wearable fabric-based RFID skin temperature monitoring patch," in *2016 IEEE SENSORS*, IEEE, 2016, pp. 1–3. Accessed: Oct. 13, 2023.

[20] G. Gonz lez-L pez, J. Romeu, I. Cair s, I. Segura, T. Ikumi, and L. Jofre-Roca, "Wireless sensing of concrete setting process," *Sensors*, vol. 20, no. 20, p. 5965, 2020.

[21] P. Kot, M. Muradov, M. Gkantou, G. S. Kamaris, K. Hashim, and D. Yeboah, "Recent advancements in non-destructive testing techniques for structural health monitoring," *Appl. Sci.*, vol. 11, no. 6, p. 2750, 2021.

[22] E. Pittella, L. Angrisani, A. Cataldo, E. Piuze, and F. Fabbrocino, "Embedded split ring resonator network for health monitoring in concrete structures," *IEEE Instrum. Meas. Mag.*, vol. 23, no. 9, pp. 14–20, 2020.

[23] X. Li, S. Xue, L. Xie, G. Wan, and C. Wan, "An off-center fed patch antenna with overlapping sub-patch for simultaneous crack and

> REPLACE THIS LINE WITH YOUR MANUSCRIPT ID NUMBER (DOUBLE-CLICK HERE TO EDIT) <

- temperature sensing," *Smart Mater. Struct.*, vol. 31, no. 9, p. 095036, 2022.
- [24] M. Wagih and J. Shi, "Wireless ice detection and monitoring using flexible UHF RFID tags," *IEEE Sens. J.*, vol. 21, no. 17, pp. 18715–18724, 2021.
- [25] L. Xie, S. Xue, Z. Yi, and G. Wan, "Double-frequency passive deformation sensor based on two-layer patch antenna," *Smart Struct. Syst. Int. J.*, vol. 27, no. 6, pp. 969–982, 2021.
- [26] Z. Yi, S. Xue, L. Xie, and G. Wan, "Detection of setting time in cement hydration using patch antenna sensor," *Struct. Control Health Monit.*, vol. 29, no. 1, Jan. 2022.
- [27] ANSYS, "HFSS version 15," <https://www.ansys.com/products/electronics/ansys-electronics-desktop>, 2013.
- [28] Z. Yi, S. Xue, L. Xie, G. Wan, and C. Wan, "Detection of Setting Time During Cement Hydration Using Multi-Electromagnetic Parameters of Patch Antenna Sensor," *IEEE Trans. Instrum. Meas.*, 2023, Accessed: Oct. 13, 2023.
- [29] Z. Yi, S. Xue, L. Xie, G. Wan, and C. Wan, "A Slotted-Patch Antenna Sensor With Higher Sensitivity for Detecting Setting Time of Cement Paste," *IEEE Trans. Instrum. Meas.*, vol. 71, pp. 1–13, 2022.
- [30] Sihvola A H, Kong J A, Effective permittivity of dielectric mixtures. :*IEEE Trans Geosci Remote Sens*, vol. 26, no.4, pp. 420-429, 1988.
- [31] S. Evans, "Dielectric properties of ice and snow-a review," *J. Glaciology*, vol. 5, pp. 773-792.
- [32] Birchak J R, Gardner C G, Hipp J E, et al. "High dielectric constant microwave probes for sensing soil moisture," *Proceedings of the IEEE*, vol. 62, no. 1, pp. 93-98, 1974.
- [33] Z. J. Sun, "Estimating volume fraction of bound water in Portland cement concrete during hydration based on dielectric constant measurement," *Mag. Concr. Res.*, vol. 60, no. 3, pp. 205–210, Apr. 2008.
- [34] B. Zhuang, G. Ramanauskaite, Z. Y. Koa, and Z.-G. Wang, "Like dissolves like: A first-principles theory for predicting liquid miscibility and mixture dielectric constant," *Sci. Adv.*, vol. 7, no. 7, p. eabe7275, Feb. 2021.
- [35] C. G. Malmberg and A. A. Maryott, "Dielectric constant of water from 0 to 100 C," *J. Res. Natl. Bur. Stand.*, vol. 56, no. 1, pp. 1–8, 1956.
- [36] Y. Li and N. Bowler, "Resonant frequency of a rectangular patch sensor covered with multilayered dielectric structures," *IEEE Trans. Antennas Propag.*, vol. 58, no. 6, pp. 1883–1889, 2010.
- [37] Types/Grade of cement. https://www.eabassoc.co.uk/cement-type-grades.php?srsltid=AfmBOoo6mimq0Q11KoM6e1TLEXIh9k1S1o5FGJ_O_uwR371FRcirggDk3